

PhysicalpropertiesandphasediagramofNaFe1−xVxAs

Guang-Yang Dai(代光阳), Xin He(何鑫), Zhi-Wen Li(李芷文), Chang-Ling Zhang(张昌玲), Lu-Chuan Shi(史鲁川), Run-Ze Yu(于润泽), Xian-Cheng Wang(望贤成), and Chang-Qing Jin(靳常青)
Citation: Chin. Phys. B, 2021, 30 (**1**): 017401. DOI: 10.1088/1674-1056/abcf95
Journal homepage: http://cpb.iphy.ac.cn; http://iopscience.iop.org/cpb

What follows is a list of articles you may be interested in

Specific heat in superconductors

Hai-Hu Wen(闻海虎)
Chin. Phys. B, 2020, 29 (**1**): 017401. DOI: 10.1088/1674-1056/ab5a3d

Cubic anvil cell apparatus for high-pressure and low-temperature physical property measurements

Jin-Guang Cheng(程金光), Bo-Sen Wang(王铂森), Jian-Ping Sun(孙建平), Yoshiya Uwatoko
Chin. Phys. B, 2018, 27 (**7**): 077403. DOI: 10.1088/1674-1056/27/7/077403

Structural phase transition, precursory electronic anomaly, and strong-coupling superconductivity in quasi-skutterudite $(Sr_{1-x}Ca_x)_3Ir_4Sn_{13}$ and $Ca_3Rh_4Sn_{13}$

Jun Luo(罗军), Jie Yang(杨杰), S Maeda, Zheng Li(李政), Guo-Qing Zheng(郑国庆)
Chin. Phys. B, 2018, 27 (**7**): 077401. DOI: 10.1088/1674-1056/27/7/077401

Topological phase diagrams and Majorana zero modes of the Kitaev ladder and tube

Yiming Wang(王一鸣), Zhidan Li(李志聃), Qiang Han(韩强)
Chin. Phys. B, 2018, 27 (**4**): 047401. DOI: 10.1088/1674-1056/27/4/047401

Quantum critical behavior in an antiferromagnetic heavy-fermion Kondo lattice system $(Ce_{1-x}La_x)_2Ir_3Ge_5$

Rajwali Khan, Qianhui Mao(毛乾辉), Hangdong Wang(王杭栋), Jinhu Yang(杨金虎), Jianhua Du(杜建华), Binjie Xu(许彬杰), Yuxing Zhou(周宇星), Yannan Zhang(张燕楠), Bing Chen(陈斌), Minghu Fang(方明虎)
Chin. Phys. B, 2017, 26 (**1**): 017401. DOI: 10.1088/1674-1056/26/1/017401

RAPID COMMUNICATION

Physical properties and phase diagram of $NaFe_{1-x}V_xAs$*

Guang-Yang Dai(代光阳)[1,2], Xin He(何鑫)[1,2], Zhi-Wen Li(李芷文)[1,2], Chang-Ling Zhang(张昌玲)[1,2], Lu-Chuan Shi(史鲁川)[1,2], Run-Ze Yu(于润泽)[1], Xian-Cheng Wang(望贤成)[1,2,†], and Chang-Qing Jin(靳常青)[1,2,3,‡]

[1] *Institute of Physics, Chinese Academy of Sciences, Beijing* 100190, *China*
[2] *University of Chinese Academy of Sciences, Beijing* 100190, *China*
[3] *Materials Research Laboratory at Songshan Lake, Dongguan* 523808, *China*

(Received 13 November 2020; revised manuscript received 24 November 2020; accepted manuscript online 2 December 2020)

We grew a series of $NaFe_{1-x}V_xAs$ ($0 \le x \le 0.03$) single crystals and performed the measurements of resistance, magnetic susceptibility, and specific heat to study the superconducting phase diagram by doping V into NaFeAs. Both the structural and the spin-density-wave (SDW) transitions are slightly suppressed by V-doping. While superconducting transition temperature is enhanced to the maximum value of ~ 15 K when the optimal doping level $x = 0.007$ and then is suppressed rapidly with further V-doping, displaying a small superconducting dome. Our results suggest that V-impurities should act as strong magnetic scattering centers which cause the sharp suppression of superconductivity in $NaFe_{1-x}V_xAs$.

Keywords: iron based superconductor, "111" type NaFeAs, V doping, phase diagram

PACS: 74.70.Xa, 74.25.Dw, 74.25.–q, 74.62.Dh **DOI:** 10.1088/1674-1056/abcf95

1. Introduction

The discovery of the superconducting $LaO_{1-x}F_xFeAs$[1] with transition temperature (T_C) of 26 K has attracted great interest in the condensed matter physics field. Soon after this discovery, the T_C was quickly enhanced to a maximum of 55 K by replacing La with Sm atoms.[2] Subsequently, several new families of iron-based superconductors were discovered successively, such as 122-type (Ba, K)Fe_2As_2,[3] 111-type LiFeAs,[4] and 11-type FeSe.[5] The parent compounds of most iron-based superconductors generally undergo a tetragonal-to-orthorhombic structural transition and a spin density wave (SDW) transition from paramagnetic to antiferromagnetic state at low temperature. By chemical doping or applying pressure, the structural and SDW transitions can be suppressed and then superconductivity is induced or enhanced.[6–14]

The parent compound NaFeAs, as a member of the "111" family, exhibits a structural transition at $T_S = 52$ K and a SDW transition at $T_{SDW} = 41$ K, respectively.[15] So far, the doping effects on the superconductivity via the substitution of Fe in NaFeAs by Co,[13] Cu,[14] Ni,[16,17] and Rh[18] atoms have been investigated, which are considered to introduce electrons into NaFeAs. With the increase of doping level x in $NaFe_{1-x}T_xAs$ (T denotes Co, Ni, Cu, and Rh), the structural/SDW transitions are gradually suppressed and dome-like doping dependence of T_C is observed. For Co-doping, the maximum T_C is 21 K with the optimal doping level $x = 0.028$. The Rh doping effect on the superconductivity of NaFeAs is almost identical to that of Co doping, and the doping effect of Ni is double that of Co if the doping level is fixed. While for the dopant Cu, the optimal T_C is 11.5 K, which is much smaller than that of Co doping. Except for the electronic doping, however, there is little research about the hole doping effect on NaFeAs and a hole-doped phase diagram for NaFeAs is still lacking. The doping effect of V has been investigated in LiFeAs,[19] which suggests that V dopants introduce hole carriers. What is more, the V dopants act as strong scattering centers and give rise to the rapid suppression of superconductivity for LiFeAs. In this work, we report the study of V doping effect on $NaFe_{1-x}V_xAs$ system. A phase diagram of $NaFe_{1-x}V_xAs$ is obtained. It is shown that V doping has a small effect on the structural and SDW transitions, while in a very narrow doping range the T_C is enhanced and then suppressed quickly, displaying a small superconducting dome. It is speculated that the strong scattering effect of V impurities dominates the suppression of T_C.

2. Experimental details

High-quality single crystals of $NaFe_{1-x}V_xAs$ have been grown using the self-flux method. The precursors of Na_3As and $Fe_{1-x}V_xAs$ were first prepared using the solid state reaction method. Na_3As was synthesized by sintering Na and As at about 600 °C for 10 h in a Ti tube filled with Ar atmosphere. $Fe_{1-x}V_xAs$ was prepared by mixing Fe, V, and As powders,

*Project supported by the National Natural Science Foundation of China and the National Key Research and Development Program of China.
†Corresponding author. E-mail: wangxiancheng@iphy.ac.cn
‡Corresponding author. E-mail: Jin@iphy.ac.cn
© 2021 Chinese Physical Society and IOP Publishing Ltd

the mixture was sealed into an evacuated quartz tube and heating to 1100 °C for 20 h. Then the Na_3As, $Fe_{1-x}V_xAs$, and As powders were mixed with the ratio of Na_3As:$Fe_{1-x}V_xAs$:As = 1 : 0.9 : 1.1. The mixture was put into an alumina oxide tube and subsequently sealed in a Nb tube and placed in an evacuated quartz tube. The quartz tube was heated to 950 °C for 20 h and then slowly cooled down to 650 °C at a rate of 3 °C/h to grow single crystals. The crystals with typical size of $4 \times 4 \times 0.1$ mm^3 can be obtained. To protect the samples from reacting with air or water, all the synthesis processes were carried out in high-purity Ar atmosphere.

The single crystals were characterized by x-ray diffraction (XRD) in the 10°–70° range on a Philips X'pert diffractometer using Cu $K\alpha$ radiation generated at 40 kV and 40 mA. The actual chemical compositions of $NaFe_{1-x}V_xAs$ single crystals were determined by energy dispersive x-ray spectroscopy (EDX). The electrical resistance was measured by a physical property measurement system (PPMS) using the four-probe method. The DC magnetic susceptibility was measured using a superconducting quantum interference device (SQUID). The measurement of specific heat was performed from 2 K to 60 K using PPMS.

3. Results and discussion

Figure 1(a) shows the XRD patterns for the selected $NaFe_{1-x}V_xAs$ single crystals. Only sharp (00l) peaks can be observed and the full width at half maximum (FWHM) is small. For the example of $NaFe_{0.988}V_{0.012}As$, the FWHM of (001) peak is about 0.04° as shown in the inset of Fig. 1(a), which indicates a high-quality of the single crystals used for the following measurements. The lattice parameter c can be obtained from the angles of these (00l) peaks and is plotted as a function of V doping level in Fig. 1(b). The c value increases with the increase of x and the amplitude of the enhancement is about 0.2% when x increases to 0.03, which suggests that V is doped into the crystal lattice of NaFeAs.

Figure 2(a) shows the temperature dependence of the *ab*-plane resistance for $NaFe_{1-x}V_xAs$ single crystals with $x \leq 0.03$. When the V-doping level is below 0.01, we can find zero resistance above 2 K. For the samples of $x = 0.012$ and 0.016, the resistance drops sharply at low temperature, implying the existence of superconductivity. However, zero resistance is not observed within experimental temperature range. If x exceeds 0.016, the superconductivity seems to be suppressed completely. Here, we define the temperature where the resistance reaches zero as T_C. It is found that T_C increases with the initial increase of x and reaches to the maximum of ~ 15 K when $x = 0.007$, then decreases with further increasing x, demonstrating a superconducting dome. After the superconductivity is completely suppressed, $NaFe_{1-x}V_xAs$ displays a semiconducting behavior at low temperature, which has been observed in $NaFe_{1-x}Cu_xAs$ with $x > 0.033$.

The V-doping dependence of T_C can also be seen in the magnetic susceptibility data as shown in Fig. 3. The temperature at which the susceptibility starts to be negative is defined as T_C^*. To clearly see the evolution of T_C^* and the superconducting volume fraction , the susceptibility data are multipled by factors as shown in the inset of Fig. 3. The susceptibility of the parent sample demonstrates the diamagnetic sign below ~ 8 K, suggesting that the superconductivity occurs with T_C^* about 8 K. The diamagnetic sign, however, is very weak. It implies that the superconductivity of NaFeAs is not bulk-like. When V-doping level x increases gradually to 0.007, T_C^* increases and the shielding fraction is enhanced correspondingly. Especially, for the 0.7%-V sample, the shielding fraction reaches 20% and thus, it becomes a bulk superconductor. When x exceeds 0.007, both T_C^* and shielding fraction decrease with further increasing x.

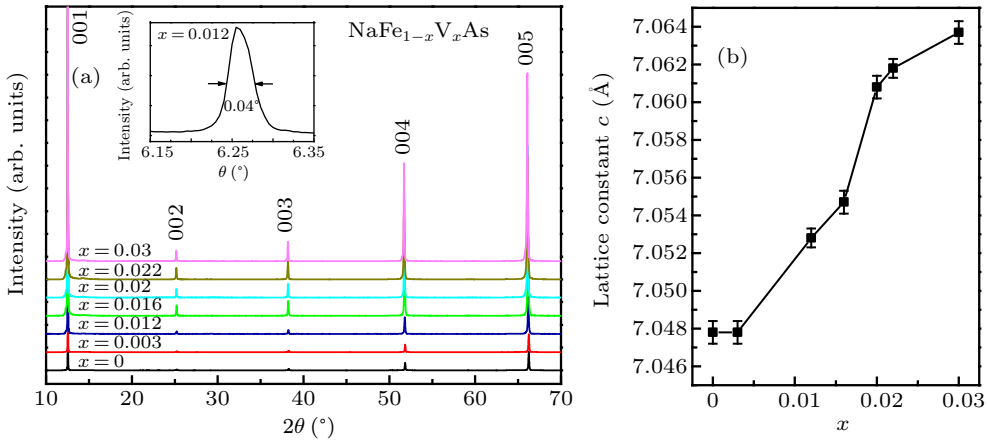


Fig. 1. (a) XRD pattern of $NaFe_{1-x}V_xAs$ single crystals, the inset shows the FWHM of about 0.04°. (b) The lattice parameter c plotted as a function of the V concentration x.

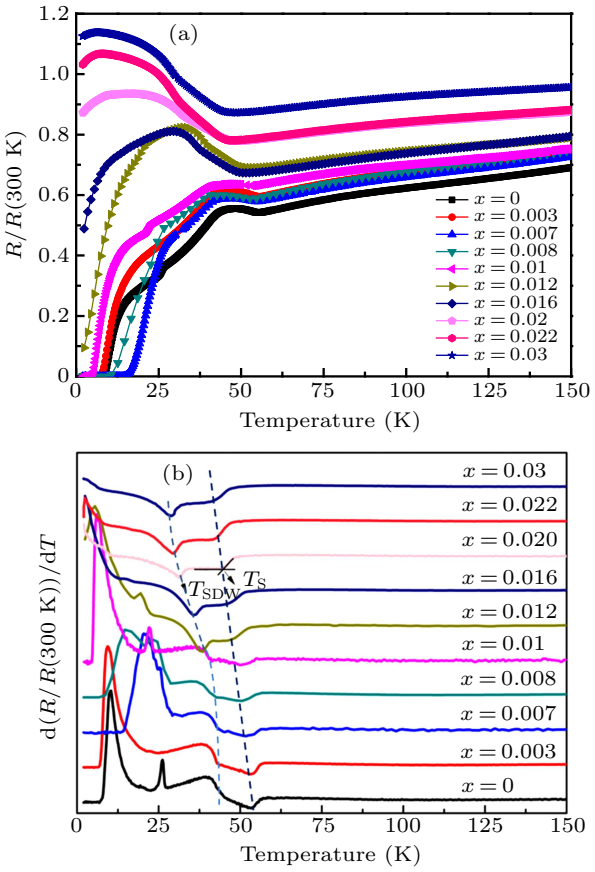


Fig. 2. (a) The normalized resistance $R/R(300\ \mathrm{K})$ as a function of temperature for the $NaFe_{1-x}V_xAs$ single crystals. (b) The derivative resistance for $NaFe_{1-x}V_xAs$ single crystals, where T_S and T_{SDW} are marked with arrows.

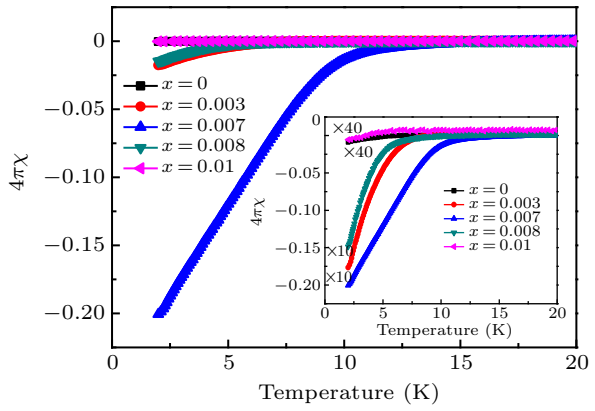


Fig. 3. Magnetic susceptibility taken at 30 Oe in ZFC mode for the superconducting samples. The inset shows the susceptibility data multiplied by some factors.

Beside the superconductivity we can explore the evolution of the structural and magnetic transitions when varying the V-doping level. The temperature derivatives of the resistances for $NaFe_{1-x}V_xAs$ samples are plotted in Fig. 2(b). The two distinct features marked by the arrows are used to determine the temperatures of structural transition T_S and SDW transition T_{SDW}.[13] It is clearly seen that both T_S and T_{SDW} shift towards low temperature when V is doped. When x is 0.03, T_S is suppressed to 42 K and T_{SDW} about 29 K. We can also determine the T_S and T_{SDW} values from the specific heat data, as seen in Fig. 4. For the 1.2%-V sample there are two kinks at 52 K and 40 K, which correspond to the structural transition and SDW transition, respectively. From the temperature derivative of the specific heat data for 2.2%-V sample we can define $T_S \sim 45$ K and $T_{SDW} \sim 31$ K, as shown in the inset of Fig. 4. The transition temperatures defined from the specific heat data agree well with the result of the resistance data.

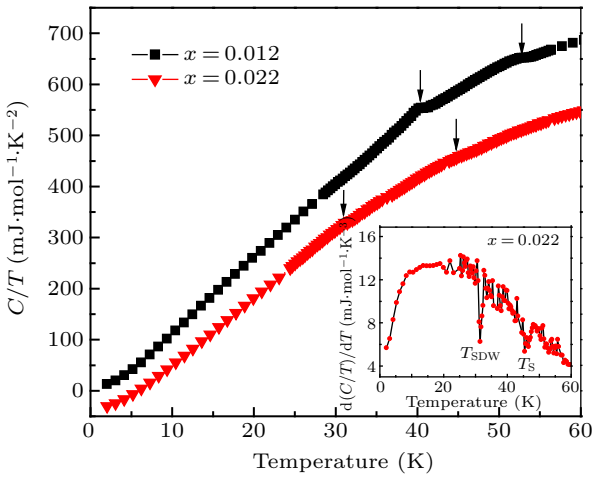


Fig. 4. Temperature dependence of the specific heat C/T of $NaFe_{1-x}V_xAs$ with $x = 0.012$ and 0.022 between 2 K and 60 K, the arrows point to the anomalies in the specific heat. The inset shows the derivative of the specific heat for the crystal with $x = 0.022$.

Finally, we plot the phase diagram of $NaFe_{1-x}V_xAs$ based on the data of resistance, magnetic susceptibility, and specific heat, as shown in Fig. 5. With the increase of the V-doping level, both the structural and SDW transitions are gradually suppressed. At the same time, T_C increases to the maximum value of ~ 15 K at the optimal doping level $x = 0.007$ and then decreases rapidly to zero when x is 0.012. We can make a comparison of V-doping behavior in iron based superconductors with other 3d transition metal doping. The Co-doping and Ni-doping are usually considered to introduce electrons into the system and T_C seems to be mainly related to the doped electron count. The substitution of one Fe atom by Co (Ni) atom would introduce one (two) extra electrons, which means that Ni-doping has the doubled effect of Co-doping if the doping level keeps the same. For Cu-doping, although it does introduce electron carriers into the system, the impurity scattering effect plays an important role on T_C suppression. Moderate Cu-doping, such as $x \sim 0.033$ for $NaFe_{1-x}Cu_xAs$[14] and $x \sim 0.13$ for $LiFe_{1-x}Cu_xAs$,[20] can cause a crossover from metallic state to semiconducting one due to Anderson localization, which suggests that Cu impurities are strong scattering centers and would suppress T_C via destroying the Cooper pairs. While V-doping effect is only studied systematically in LiFeAs system. Contrast with Co, Ni, and Cu, hope carriers are introduced into LiFeAs by V-doping. In addition, V impurities are proved to be magnetic and have stronger electron scattering ability than Cu impurities, which is the cause

that T_C is suppressed with a much larger rate of 7 K per 1%-V[19] than the rate of 1 K per 1%-Co[21] and 1.9 K per 1%-Cu[20] in LiFeAs system. Here, both T_C and shielding fraction of $NaFe_{1-x}V_xAs$ are enhanced when 0.7%-V is doped, suggesting that V-doping introduces hole carriers into NaFeAs. However, T_C decreases rapidly after the optimal doping level of 0.007 and disappears completely at $x = 0.012$, from which the T_C suppression rate can be calculated to be about 30 K per 1%-V in NaFeAs system. For the Co-doped NaFeAs system, the optimal doping level is 3% with the maximum $T_C \sim 21$ K and T_C decreases to zero when the doping level is about 10%. That is, the T_C is suppressed with a rate about 3 K per 1%-Co in $NaFe_{1-x}Co_xAs$ system. The suppression rate can also be coarsely calculated from the superconducting phase diagram of $NaFe_{1-x}Cu_xAs$ to be ~ 5.5 K per 1%-Cu. The large suppression rate of T_C by V doping means that the magnetic impurity scattering effect dominates the suppression of T_C in NaFeVAs. In addition, the structural and SDW transitions are only slightly suppressed by V-doping if compared with that of Co- or Cu-doping. The effect of V-doping on structural and SDW transitions in NaFeAs is similar to the behavior of Cr-doping in $BaFe_2As_2$ system.[22]

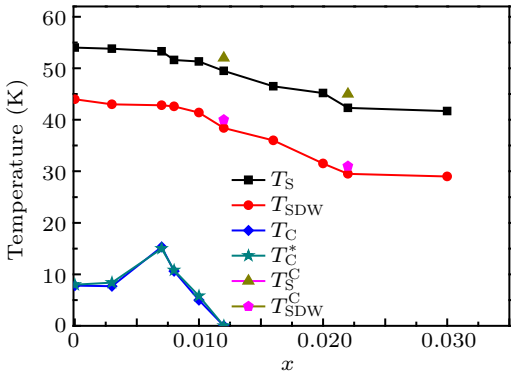


Fig. 5. Phase diagram of $NaFe_{1-x}V_xAs$. T_S, T_{SDW}, and T_C are determined from the resistance, T_C^* is determined from the magnetic susceptibility, T_S^C and T_{SDW}^C are determined from the specific heat.

4. Conclusion

In summary, we have grown a series of $NaFe_{1-x}V_xAs$ single crystals to study the V-doping effect on the superconductivity of NaFeAs via resistance, magnetic susceptibility, and specific heat measurements. The phase diagram of $NaFe_{1-x}V_xAs$ was obtained. V doping has a small effect on the structural and magnetic transitions. T_C increases from ~ 8 K of the parent NaFeAs to the maximum value of ~ 15 K at the optimal doping level $x = 0.007$, and then decreases rapidly to zero when $x = 0.012$. T_C is suppressed with a large rate about 30 K per 1%-V in NaFeAs system, which suggested that V impurities act as strong scatter centers.

References

[1] Kamihara Y, Watanabe T, Hirano M and Hosono H 2008 *J. Am. Chem. Soc.* **130** 3296

[2] Ren Z A, Lu W, Yang J, Yi W, Shen X L, Li Z C, Che G C, Dong X L, Sun L L, Zhou F and Zhao Z X 2008 *Chin. Phys. Lett.* **25** 2215

[3] Rotter M, Tegel M and Johrendt D 2008 *Phys. Rev. Lett.* **101** 107006

[4] Wang X C, Liu Q Q, Lv Y X, Gao W B, Yang L X, Yu R C, Li F Y and Jin C Q 2008 *Solid State Commun.* **148** 538

[5] Hsu F C, Luo J Y, Yeh K W, Chen T K, Huang T W, Wu P M, Lee Y C, Huang Y L, Chu Y Y, Yan D C and Wu M K 2008 *P. Natl. Acad. Sci. USA* **105** 14262

[6] Luetkens H, Klauss H H, Kraken M, Litterst F J, Dellmann T, Klingeler R, Hess C, Khasanov R, Amato A, Baines C, Kosmala M, Schumann O J, Braden M, Hamann-Borrero J, Leps N, Kondrat A, Behr G, Werner J and Buchner B 2009 *Nat. Mater.* **8** 305

[7] Zhao J, Huang Q, de la Cruz C, Li S L, Lynn J W, Chen Y, Green M A, Chen G F, Li G, Li Z, Luo J L, Wang N L and Dai P C 2008 *Nat. Mater.* **7** 953

[8] Chen H, Ren Y, Qiu Y, Bao W, Liu R H, Wu G, Wu T, Xie Y L, Wang X F, Huang Q and Chen X H 2009 *Europhys. Lett.* **85** 17006

[9] Nandi S, Kim M G, Kreyssig A, Fernandes R M, Pratt D K, Thaler A, Ni N, Bud'ko S L, Canfield P C, Schmalian J, McQueeney R J and Goldman A I 2010 *Phys. Rev. Lett.* **104** 057006

[10] Torikachvili M S, Bud'ko S L, Ni N and Canfield P C 2008 *Phys. Rev. Lett.* **101** 057006

[11] Igawa K, Okada H, Takahashi H, Matsuishi S, Kamihara Y, Hirano M, Hosono H, Matsubayashi K and Uwatoko Y 2009 *J. Phys. Soc. Jpn.* **78** 025001

[12] Matsubayashi K, Katayama N, Ohgushi K, Yamada A, Munakata K, Matsumoto T and Uwatoko Y 2009 *J. Phys. Soc. Jpn.* **78** 073706

[13] Wang A F, Luo X G, Yan Y J, Ying J J, Xiang Z J, Ye G J, Cheng P, Li Z Y, Hu W J and Chen X H 2012 *Phys. Rev. B* **85** 224521

[14] Wang A F, Lin J J, Cheng P, Ye G J, Chen F, Ma J Q, Lu X F, Lei B, Luo X G and Chen X H 2013 *Phys. Rev. B* **88** 094516

[15] Chen G F, Hu W Z, Luo J L and Wang N L 2009 *Phys. Rev. Lett.* **102** 227004

[16] Wang W Y, Song Y, Cao C D, Tseng K F, Keller T, Li Y, Harriger L W, Tian W, Chi S X, Yu R, Nevidomskyy A H and Dai P C 2018 *Nat. Commun.* **9** 3128

[17] Cheung S C, Guguchia Z, Frandsen B A, Gong Z Z, Yamakawa K, Almeida D E, Onuorah I J, Bonfa P, Miranda E, Wang W Y, Tam D W, Song Y, Cao C D, Cai Y P, Hallas A M, Wilson M N, Munsie T J S, Luke G, Chen B J, Dai G Y, Jin C Q, Guo S L, Ning F L, Fernandes R M, De Renzi R, Dai P C and Uemura Y J 2018 *Phys. Rev. B* **97** 224508

[18] Steckel F, Roslova M, Beck R, Morozov I, Aswartham S, Evtushinsky D, Blum C G F, Abdel-Hafiez M, Bombor D, Maletz J, Borisenko S, Shevelkov A V, Wolter A U B, Hess C, Wurmehl S and Büchner B 2015 *Phys. Rev. B* **91** 184516

[19] Xing L Y, Shi X, Richard P, Wang X C, Liu Q Q, Lv B Q, Ma J Z, Fu B B, Kong L Y, Miao H, Qian T, Kim T K, Hoesch M, Ding H and Jin C Q 2016 *Phys. Rev. B* **94** 094524

[20] Xing L Y, Wang X C, Deng Z, Zhang S J, Feng S M, Li W M, Liu Q Q and Jin C Q 2015 *Int. J. Mod. Phys. B* **29** 1542023

[21] Dai Y M, Miao H, Xing L Y, Wang X C, Wang P S, Xiao H, Qian T, Richard P, Qiu X G, Yu W, Jin C Q, Wang Z, Johnson P D, Homes C C and Ding H 2015 *Phys. Rev. X* **5** 031035

[22] Zhang R, Gong D, Lu X, Li S, Laver M, Niedermayer C, Danilkin S, Deng G, Dai P and Luo H 2015 *Phys. Rev. B* **91** 094506